Title

Mice lacking substance P have normal bone modeling but diminished bone formation, increased resorption, and accelerated osteopenia with aging

Authors

Wang, Liping
Hou, Saiyun
Sabsovich, Ilya
et al.

Publication Date

2021-03-01

DOI

10.1016/j.bone.2020.115806

Peer reviewed

HHS Public Access

Author manuscript

Bone. Author manuscript; available in PMC 2022 March 01.

Published in final edited form as:

Bone. 2021 March ; 144: 115806. doi:10.1016/j.bone.2020.115806.

Mice lacking substance P have normal bone modeling but diminished bone formation, increased resorption, and accelerated osteopenia with aging

Liping Wang[a], **Saiyun Hou**[a], **Ilya Sabsovich**[a], **Tian-Zhi Guo**[a], **Tzuping Wei**[a], **Wade S. Kingery**[a,*]

[a]Palo Alto Veterans Institute for Research, Veterans Affairs Palo Alto Health Care System, Palo Alto, California

Abstract

Substance P (SP) is a sensory neuropeptide that is expressed by the neurons innervating bone. There is considerable evidence that SP can regulate bone cell function *in vitro*, but it is unclear whether SP modulates bone modeling or remodeling *in vivo*. To answer this question we characterized the bone phenotype of mice with deletion of the *Tac1* gene expressing SP. The phenotypes of 2-month-old and 5-month-old SP deficient mice and their wildtype controls were characterized by using μCT imaging, static and dynamic bone histomorphometry, and urinary deoxypyridinoline cross-links (DPD) measurement. No differences in bone phenotypes were observed between the 2 strains at 2 months of age. By 5 months both the wildtype and SP deficient mice had developed cancellous osteopenia, but relative to the wild-type mice the SP deficient mice had significantly greater cancellous bone loss. The SP deficient mice also exhibited decreased bone formation, increased osteoclast number, and increased urinary DPD levels. Cortical defect early repair was delayed in 5-month-old mice lacking SP. Collectively, these findings indicate that SP signaling is not required for bone modeling, but SP signaling reduces age-related osteopenia and accelerates cortical defect reparation, data supporting the hypothesis that SP is an anabolic physiologic regulator of bone metabolism.

Keywords

substance P; bone; osteopenia; aging; bone remodeling

1. Introduction

Bone modeling and remodeling play crucial roles in skeletal development and renewal. Bone modeling describes the process of shaping bone by the independent actions of osteoblasts

*Corresponding Author: Wade Kingery, M.D., PAVIR (151P), 3801 Miranda Ave, Palo Alto, CA 94304, Phone: 650-207-3733, wkingery@stanford.edu.

Conflict of interest: The authors have no conflict of interests with this work.

and osteoclasts that are not necessarily coupled anatomically or temporally. Modeling defines skeletal development and growth, but continues throughout life, contributing to the periosteal expansion. Bone remodeling is a constant process in the adult skeleton involving the sequential activity of osteoclasts and osteoblasts linked in a remodeling unit, and it's importance increases with aging. Cancellous bone remains relatively stable after peak bone mass is achieved, until increased resorptive activity and reduced bone formation triggers age-related bone loss.

Due to the abundant sensory innervation of bone [1], the possible neuro-regulation of bone modeling and remodeling has become a research focus. The neuropeptides substance P (SP) and calcitonin gene-related peptide (CGRP) are synthesized in sensory neurons and released from their unmyelinated axon terminals in bone. Familial dysautonomia is a hereditary autosomal recessive disease characterized by sensory unmyelinated axon loss, impaired neuropeptide signaling, and reduced CGRP content [2,3]. Interestingly, these patients also develop osteopenia with bone fragility, and it has been proposed that neuropeptide-osseal signaling critically contributes to skeletal integrity[4].

Previously we used high-dose capsaicin treatments to selectively destroy unmyelinated sensory neurons in skeletally mature 10-month-old rats, with subsequent depletion of SP and CGRP in the peripheral nerves and metaphyseal bone [5]. Loss of sensory neuropeptide signaling inhibited new bone formation and stimulated resorption, resulting in trabecular thinning, loss of bone mass, and impaired skeletal intergrity. Substance P and CGRP perform a variety of efferent functions in peripheral tissues and we postulated that these neurotransmitters are also key regulators of bone metabolism. Furthermore, we previously observed that unilateral sciatic nerve denervation in skeletally mature rats triggered a loss of trabecular bone in the bilateral hindlimbs, which was further exacerbated by treating the rats with an SP NK_1 receptor antagonist [6], Weight-bearing in the contralateral hindlimb was actually increased after sciatic nerve transection, but SP content in the contralateral proximal tibia was reduced and neurogenic extravasation responses were impaired, evidence of a transmedian loss of SP signaling. Collectively, these data support the hypothesis that neuropeptide signaling support normal bone mass in the mature skeleton.

We also previously demonstrated that both the SP neurokinin 1 receptor (NK1) and the CGRP calcitonin receptor-like receptor (CRLR) and receptor activity modifying protein 1 (RAMP1) receptors are expressed on mouse bone marrow stromal cells (BMSCs) and bone marrow macrophages (BMMs) [7, 8]. Furthermore, both SP and CGRP stimulated BMSC osteoblastic differentiation and mineralization *in vitro*. SP treatment of BMMs facilitated receptor activator of nuclear factor-κB ligand (RANKL) induced osteoclastogenesis and resorption activity *in vitro*, but conversely, CGRP inhibited RANKL induced BMM osteoclastogenesis and bone resorption[7, 8].

The *in vitro* osteogenic effects of CGRP on bone marrow stromal cells concurred with observations that 6 month-old CGRP deficient mice exhibit decreased bone formation and accelerated osteopenia with aging [9]. Surprisingly, the CGRP inhibitory effects we observed for BMM osteoclastogenesis and bone resorption *in vitro* did not replicate the results of *in vivo* investigations in CGRP deficient mice. Mice lacking CGRP did not differ

in osteoclast numbers, osteoclast surface, and urinary deoxypyridinoline cross-links (DPD) levels when compared with wildtype mice [9].

Collectively, the above data suggest that sensory peptidergic signaling is a physiologic activator of bone formation and inhibitor of bone resorption. Capsaicin lesioning of both SP and CGRP sensory innervation caused reduced bone formation, trabecular bone volume, and increased in osteoclast numbers and bone resorption in skeletally mature rats[5]. Studies in mice lacking CGRP demonstrated that CGRP contributes to bone formation and trabecular bone volume in 6 months old mice, but had no effect on bone resorption *in vivo* [9]. These results suggest that the increase in bone resorption observed with capsaicin lesioning of unmyelinated sensory neurons could be attributable to SP inhibitory effects on BMM osteoclast differentiation and resorption activity, although we observed the opposite with BMM cell culture experiments [8]. To answer this question and to characterize the physiologic role of SP in bone formation and remodeling, in current study we characterized the bone phenotypes of 2 and 5 month-old mice with a targeted deletion of the *Tac1* gene expressing SP [10]. The role of SP signaling in cortical bone defect healing was also investigated.

2. Methods

2.1. Animals

These experiments were approved by the Institutional Animal Care and Use Committee at the Palo Alto Veterans Affairs Medical Center. Substance P deficient mice (B6.Cg-Tac1^{tm1Bbm}/J) that are homozygous null for the *Tac1* gene were purchased from Jackson Laboratory, Bar Harbor ME (stock number 004103). These substance P deficient mice are of normal size, fertile, and do not display any health or behavioral abnormalities [10]. Substance P is undetectable in these mice and there is a modest reduction in nociceptive response to moderate/intense pain stimuli. The SP deficient mice are congenic on a C57BL/6J background, so the C57BL/6J strain (stock number 000664) was used for controls (wildtype). Mice were kept under pathogen-free conditions in cages maintained at 22°C with a 12 h alternating light and dark cycle. Food and water were provided *ad libitum*. All mice were fed Teklad lab rodent diet 2018 (Harlan Laboratories, Indianapolis, IN) containing 1.0% calcium, 0.7% phosphorus, and 1.5 IU/g vitamin D3. Data collection was conducted blind to group assignment.

Motor behavior and morphologic phenotypes were evaluated in the SP deficient and wildtype mice. To evaluate spontaneous locomotor activity the mice were individually placed in clear plastic monitoring chambers measuring 72 x 32 x 32 cm. While in the chamber the mice were fed and watered *ad libitum* and the floor was covered in soft bedding. The chamber contained 7 sets of photoelectric sensors evenly spaced along the length of the chamber for monitoring locomotor activity (San Diego Instruments, San Diego, CA). Total grid crossing activity was recorded as the number of times the mouse blocked the photoelectric sensors during a 24-hour monitoring session. The testing room was kept on a 10 hours light and 14 hours dark cycle with the room temperature maintained at 23°C. Motor strength and coordination was evaluated using a rotorod assay (IITC, Life Sciences Instruments, Woodland Hills, CA) rotating at 10 rpm. The mice underwent 3 training

sessions to learn to remain on the rod for 60 seconds. The mice were weighed *in vivo* and tibia length was measured *ex vivo* using calipers.

2.2. Culture of osteoblast- and osteoclast-like cells

Mouse MC3T3-E1 and Raw 264.7 cells from American Type Culture Collection (ATCC, Manassas, VA) were maintained in growth medium, containing αMEM (Invitrogen, Carlsbad, CA), 10% FBS, and 1% penicillin and streptomycin. Raw 264.7 cells were supplemented with 50 ng/ml RANKL (R&D Systems, Minneapolis, MN) for 4 days to stimulate osteoclastic differentiation.

2.3. Immunofluorescence Confocal Microscopy

The MC3T3-E1 cells were seeded on coverslips and at 3 days post-seeding they were immunostained for alkaline phosphatase and the SP NK1 receptor. The RAW 264.7 cells were also seeded on coverslips and at 5 days post-seeding were stained for tartrate-resistant acid phosphatase (TRAP) and NK1 receptor. Cells were prepared for immunostaining by fixation in 3.7% (V/V) formaldehyde for 20 min at room temperature and then permeabilized with ice-cold alcohol for 5 min [11]. To block nonspecific staining the cells were pre-incubated in 5% FBS with 1% bovine serum albumin for 60 min at room temperature. Then, the cells were incubated overnight at 4°C with goat polyclonal antibodies against the NK1 receptor (1:50 dilution, Santa Cruz Biotechnology, Dallas, TX) and mouse monoclonal antibodies against alkaline phosphatase (1:50 dilution, R&D Systems, Minneapolis, MN) or the rabbit polyclonal antibody against TRAP (1:50 dilution, Santa Cruz Biotechnology, Dallas, TX). Cells were then treated for 1 h at room temperature with the Texas-Red and FITC-conjugated secondary antibodies in 1:200 dilutions (Santa Cruz Biotechnology, Dallas, TX). Control slides were stained with only the secondary antibody. A Zeiss ISM 510 META laser scanning confocal microscope (Carl Zeiss, Jena Germany) for visualizing immunostained cells.

2.4. Real time PCR

To detect NK1 receptor gene (*Tacr1*) expression in MC3T3-E1 and RAW 264.7 cells, the cells were grown in 6 well plates and the total RNA extracted using the RNeasy Mini Kit (Qiagen, Hilden, Germany) on days 3, 7, and 14 post-seeding for MC3T3-E1 cells and on days 4 and 7 post-seeding for RAW 264.7 cells. Using the iScript cDNA Synthesis Kit (BioRad, Hercules, CA), cDNA (20 μL final volume) was synthesized from 1 μg RNA and real time PCR reactions were conducted in a volume of 4 μl using the SYBR Green PCR master mix (Applied Biosystems, Foster City, CA). The primer pair of *Tacr1* sense and antisense was specific for a 156-bp fragment of NK1 receptor transcripts (sense: 5'-gaaggctatcctcggtttcc-3'; antisense: 5'-tgtggctgagaatgacttcg-3'). The primer pair for 18S was specific for a 323-bp fragment (sense: 5'-aggaattgacggaagggcac-3'; (antisense); 5'-gtgcagccccggacatctaag-3'). The data from real time PCR experiments were analyzed by the comparative method as described in the ABI prism 7900 system manual.

2.5. Age-related bone loss in substance P deficient mice

Age-related bone changes were evaluated in 2- and 5 month-old groups of wildtype and SP deficient mice (n = 15 per cohort). The mice were subcutaneously injected twice with calcein (10 mg/kg) at 7 and 2 days before necropsy. Prior to euthanizing the mice, urine was collected over a 24 h period in metabolic cages, then under isoflurane anesthesia 1 ml of blood was collected by transcardial puncture, and then the mice were euthanized by CO2 inhalation. The right tibia and fourth lumbar vertebrae were harvested and stored in 70% alcohol at 4°C for μCT scanning and histomorphometry.

2.6. μCT analysis

Cancellous bone was evaluated at proximal tibia and cortical bone was examined at the tibial-fibular junction by μCT scanning (Viva CT 40, Scanco Medical AG, Basserdorf, Switzerland). The CT scans were reconstructed in 2048 x 2048-pixel matrices for the proximal tibia samples while tibial-fibular CT images were reconstructed in 1024 x 1024-pixel matrices and stored in 3-D arrays.

In the proximal tibia, 100 slices of 10.5μm thickness (10.5-μm isotropic voxel size) encompassing 1mm in the proximal tibia were evaluated, starting at the end of the metaphysis growth plate bridge. On each CT slice the region of interest was manually outlined, excluding the primary spongiosa, and extending distally from the growth plate. At the tibial-fibular junction, 25 transverse CT slices were obtained, each 21 μm thick totaling 0.525 mm in length (21-μm isotropic voxel size).

The μCT parameters used in the proximal tibia cancellous bone were threshold = 252, sigma = 0.8, support = 1. The bone volume fraction (BV/TV, %), trabecular number (Tb.N, mm^{-1}), trabecular thickness (Tb.Th, μm), trabecular separation (Tb.Sp,μm), and connectivity density (ConnD, mm^{-3}) were measured in three dimensions using direct 3D morphometry based on the distance transformation without assumptions regarding the underlying bone architecture [12, 13].

The μCT parameters used in the tibial-fibular cortical bone were threshold = 350, sigma = and support = 1. The total cross-sectional area (Tt.Ar, mm^2), cortical bone area (B.Ar, mm^2), cortical thickness (Ct.Th, μm), medullary area (Me.Ar), and bone perimeter (B.Pm, mm) were measured. The relative cortical bone area (B.Ar/T.Ar, %) was calculated.

2.7. Bone histomorphometry

Histomorphometric evaluation of cancellous bone was performed in the right proximal tibia and the L4 vertebra. Bones were dehydrated in graded concentrations of alcohol, embedded undecalcified in MMA, and then sectioned using a Leica/Jung 2255 microtome (Leica Biosystems, Wetzlar, Germany) into 4- and 8-μm-thick sections. The proximal tibia was sagitally sectioned and the L4 vertebral body was coronally sectioned. The 4 μm sections were stained with toluidine blue for collection of bone mass and architecture data with the light microscope. The 8 μm sections were left unstained for measurements of fluorochrome-based indices.

Static and dynamic histomorphometry was performed using a semiautomatic image analysis system (Bioquant, Nashville, TN) attached to a Nikon Eclipse 80i microscope (Nikon, Tokyo, Japan). Histomorphometric analysis was performed in the secondary spongiosa of the proximal tibia and in the central vertebra. The region of interest (ROI) for proximal tibia trabecular bone was created from 0.2 mm to 1.7 mm proximal to the growth plate. A counting window containing only trabecular bone and measuring 1.4 mm x 1.5 mm was created for vertebral histomorphometric analysis. Measurements for cancellous bone included total tissue area (T.Ar), cancellous bone area (B.Ar), cancellous bone perimeter (B.Pm) and number of osteoclasts per bone surface (N.Oc/BS, mm^{-1}). These static measurements were used to calculate cancellous bone volume (BV/TV, %), trabecular number (Tb.N, mm^{-1}), trabecular thickness (Tb.Th, μm) and trabecular separation (Tb.Sp, μm). Dynamic measurements for cortical and cancellous bone included single- (sL.Pm) and double-labeled perimeter (dL.Pm) and interlabel width (Ir.L.Wi). Interlabel widths were averaged from all double label widths. Mineralizing surface per bone surface (MS/BS, %) and mineral apposition rate (MAR, μm/yr) were measured in unstained sections under UV light and used to calculate surface-based bone formation rate (BFR/BS, $\mu m^3/\mu m^2/yr$) according to Parfitt et al [14].

2.8. Tibia cortical bone defect model

The effect of SP signaling on bone reparation was studied in a cortical bone defect model [15]. In the mid-tibia of wildtype and SP deficient 5-month-old male mice a straight longitudinal skin incision 5 mm long was made over the anterior proximal tibia and the surface of the tibia was exposed. Using a 1 mm drill, a hole was drilled through cortical bone and bone marrow, without damaging the opposite cortex. This injury models the healing response of a stabilized long bone fracture and occurs through intramembranous ossification [15]. After surgery the wound was closed, the mice were returned to their cages, and at 1, 2, or 3 weeks post-surgery the mice were euthanized and the tibia collected and were fixed in 70% ethanol, and then embedded undecalcified in methylmethacrylate. Five-micrometer-thick coronal sections of the tibia defect were cut with a Leica/Jung 2255 microtome (Leica Biosystems, Wetzlar, Germany) and then calcium labeling was performed utilizing a von Kossa stain kit (Abcam, Cambridge, United Kingdom). Sections were analyzed using a semiautomatic image analysis system (Bioquant, Nashville, TN) attached to a Nikon Eclipse 80i microscope (Nikon, Tokyo, Japan) equipped with transmitted and fluorescent lights. Bone volume within the bone marrow cavity was calculated as a percentage of the area of within the bone marrow cavity directly below the defect (Me. BV/TV%). Bone volume within the cortical defect was calculated as a percentage of the area of the cortical defect (Ct. BV/TV%).

2.9. Biochemical DPD assay and serum chemistry analysis

To quantify osteoclastic bone resorption, we measured the urinary excretion of deoxypyridinoline cross-links (DPD) with a Pyrilinks-D ELISA (Quidel Corporation, Mountain View, CA, USA). Values are expressed relative to creatinine concentrations as determined by a standardized colorimetric assay using Quidel alkaline picrate.

The serum concentrations of total calcium, inorganic phosphorus, sodium, potassium, chloride, glucose, blood urea nitrogen, creatinine, albumin, total protein, cholesterol, alkaline phosphatase, alanine transaminase, aspartate transaminase, γ-glutamyl transpedptidase, total bilirubin, and creatinine phosphokinase were determined using a Beckman LX 20 Analyzer (Beckman Coulter, Brea, CA).

2.10. Statistical analysis

Statistical analysis was performed using a one-way repeated measures analysis of variance with Sidak multiple comparisons test for post hoc contrasts (Prism 5, GraphPad Software, San Diego, CA). To assess the overall influence of age and genotype on skeletal morphology assessed by μCT scanning, the percent change in each μCT parameter between 2 and 5 months of age was expressed as mean percent difference (MPD) of aging, and computed using a formula: (5 month $_{mean}$ − 2 month $_{mean}$) / 2 month $_{mean}$ x 100, derived from the values of each age cohort.

3. Results

3.1. *No evidence of skeletal unloading or altered serum chemistry in SP* deficient *mice*

There was no evidence of skeletal unloading or metabolic abnormalities in the SP deficient mice. The 2 month-old mice lacking SP did exhibit slightly diminished spontaneous 24-hour grid crossing exploratory behavior, compared to wildtype controls, but this was not significant at 5 months of age (Fig. 1A). Furthermore, body weight and rotarod motor function was unchanged in the SP deficient mice versus the wildtype mice at 2 and 5 months (Fig. 1B, D) and there were no serum chemistry differences between groups, except the 5 month-old mice lacking SP had slightly reduced serum cholesterol levels (Table 1, 93 ± 3 mg/dL for SP deficient vs 110 ± 2 mg/dL for wildtype, $p<0.001$). Tibia bone length was equal between groups at 2 and 5 months of age, indicating that SP signaling was not required for normal bone modeling (Fig. 1C).

3.2. Bone cells express substance P neurokinin 1 receptors

To answer the question of whether bone cells are potential targets for substance P signaling we tested for the presence of neurokinin 1 receptors in osteoblast-like (MC3T3-E1) and osteoclast-like (RAW 264.7 cells) as illustrated in Figure 2. Alkaline phosphatase and TRAP are selective markers of osteoblast- and osteoclast-like cells, respectively. Immunofluorescence confocal microscopy revealed that the osteoblastic MC3T3-E1 cells co-expressed alkaline phosphatase (Fig. 2A; green) and neurokinin 1 receptors (Fig. 2B; red) and the osteoclastic RAW 264.7 cells co-localized TRAP (Fig. 2D; green) with neurokinin 1 receptors (Fig. 2E; red). Immunofluorescent signals for neurokinin 1 receptors were detected in the cytoplasm and on the plasma membrane in both cell lines.

Neurokinin 1 receptor mRNA expression (Tachykinin Receptor 1, TACR1) in MC3T3-E1 cells and in RAW 264.7 cells was quantified using real time PCR to determine whether TACR1 expression is related to the status of bone cell growth *in vitro*. After being normalized to 18S, no temporal differences were observed in TACR1 expression over time

in the MC3T3-E1 cultures, however, TACR1expression was significantly elevated in RAW 264.7 cells on day 7 relative to day 4 post-seeding (data not shown).

3.3. Effects of SP deficiency on age-related changes in skeletal phenotype

Figure 3 illustrates that there were no differences in proximal tibia BV/TV, Tb.N, Tb.Th, Tb.Sp and tibial-fibular junction Ct.Th between 2 months old SP deficient mice and the age-matched controls. Between 2 and 5 months of age wildtype mice had diminished Tb.N, and Conn.D and increased TB.Sp, while SP deficient 5 month old mice had reduced BV/TV, Tb.N, and Conn.D, and increased Tb.Sp. At 5 months of age the SP deficient mice, relative to age-matched wildtype mice, had decreased BV/TV and Tb.Th, with increased Tb.Sp.

Table 2 presents the differences between SP deficient and wildtype mice in age-related trabecular bone loss between 2 and 5 months of age. There was a greater loss of proximal tibia cancellous bone in SP deficient mice than in wildtype mice (−30.7% vs −9.4% reduction in BV/TV with aging, respectively, $p < 0.001$). The SP deficient mice also exhibited greater age-related reductions in Tb.N, Tb.Th, and Conn.D, and a greater increase in Tb.Sp than the wildtype mice. At the tibial-fibular junction no differences were observed between SP deficient and wildtype mice in age-related increases in Tt.Ar, Me.AR, and decreases in B.Ar/Tt.Ar. The SP deficient mice did exhibit a greater increase in diaphyseal B.Pm with aging than the wildtype controls ($p < 0.05$). Collectively these results indicate that SP deficient mice have greater age-related trabecular bone loss than wildtype mice.

3.4. Effects of SP deficiency on bone remodeling

To characterize the effects of aging on bone remodeling activity in SP-deficient mice, we assessed changes in bone formation rate and osteoclast numbers at the trabecular bone surfaces in the proximal tibia (Fig. 4A,B) and L4 vertebral body (Fig. 4C,D) between the ages of 2 and 5 months. An age-related decrease in cancellous bone formation rate and an age-related increase in osteoclastogenesis, as indicated by osteoclast numbers (N.Oc/BS), were observed in SP deficient mice, but not in wildtype controls. At the age of 5 months, cancellous bone formation rate was significantly lower whereas osteoclast number was significantly higher in the SP deficient mice than in the age-matched controls. Bone resorption was also studied by measuring the total urinary DPD levels. We observed a reduction in urinary DPD levels in both strains from 2 to 5 months of age (Fig. 4E). However, at both 2 and 5 months of age the urinary DPD levels in the SP deficient mice were significantly higher than in the age-matched wildtype controls. Collectively, these data demonstrate that at 5 months of age the SP deficient mice exhibit diminished trabecular bone formation, increased osteoclast numbers, and increased bone resorption.

3.5. Effects of SP deficiency on cortical bone defect reparation

Regenerating woven bone appeared in the marrow area within 1 week after cortical defect surgery in SP deficient and wildtype control mice and persisted for at least 3 weeks post surgery (Fig. 5A,C). The bony callous volume within bone marrow cavity zone (Me. BV/TV) at 1 week post surgery was significantly less in the SP deficient mice than in wildtype mice. Lamellar bone and periosteal fibrous tissue appeared at the cortical bone defect region at 2 and 3 weeks post surgery (Fig. 5B,C). The bone callous volume within

cortical defect zone (Ct. BV/TV) was reduced in the SP deficient mice compared to the wildtype controls at both 2 and 3 weeks post surgery. These results indicate that SP deficient mice had delayed cortical bone repair after bone and marrow injury.

4. Discussion

There has been some controversy about whether bone cells express SP NK1 receptors on their plasma membranes. Previous investigators failed to observe NK1 receptor mRNA expression in human periosteum-derived osteoblastic cell lines or human osteosarcoma-derived cell lines [16]. Another study observed that NK1 receptor mRNA was not present in rat calvarial primary osteoblastic cells until 14 days after seeding, consistent with the delayed development of SP stimulatory effects on osteoblastic bone formation[17]. Contrariwise, other studies have observed NK1 receptors in rat bone[18], rat primary osteoblastic cell cultures[19], and mouse induced pluripotent stem cells cultured in osteoblastic differentiation medium[20]. A recent study observed abundant immunostaining of NK1 receptors on osteoblast-like cells derived from mouse diaphysis bone chips and on RANKL stimulated BMMs that had differentiated into osteoclast-like cells [21].

Bone progenitors cells (BMSCs) originate in the bone marrow, which is densely innervated by unmyelinated neuropeptide expressing neurons [22]. Bone marrow stromal cell differentiation progresses through 3 stages of osteogenic cellular activities: proliferation, matrix maturation, and mineralization [8]. Previously we observed that mouse BMSCs express NK1 receptor mRNA at all phases of cell differentiation, and observed co-localized alkaline phosphatase and NK1 receptor immunostaining in BMSCs [8]. We also previously demonstrated NK1 mRNA expression in BMMs and observed NK1 and TRAP co-staining in BMMs [8]. Now we confirm and extend these findings by demonstrating NK1 receptor and alkaline phosphatase co-staining in the cytoplasm and on the plasma membrane of MC3T3-E1 mouse osteoblast-like cells (Fig.2A-C). In addition, we observed co-localized NK1 and TRAP immunostaining in the cytoplasm and cell membrane of RANKL stimulated RAW264.7 cells that had differentiated into multinucleated osteoclasts (Fig. 2B-F). Furthermore, we observed that NK1 receptor mRNA was stably expressed over 14 days post seeding in the MC3T3-E1 cell line and that NK1 receptor expression increased over time in the RAW 264.7 cell line.

To determine whether SP signaling contributed to skeletal integrity during bone development and during aging, we utilized SP deficient transgenic mice [10]. As the cancellous bone volume in C57BL6/6J mice peaks by 2 months of age [23, 24], we used μCT to compare the bone phenotypes of SP deficient mice and wildtype controls at the ages of 2 and 5 months and found age- and genotype-related changes at skeletal architecture that differed in a compartment-dependent fashion (Fig.3, Table 2). No differences were observed between the skeletal phenotypes of the wildtype and SP deficient mice at 2 months of age (Fig.3, Table 2). These results are in contrast to a previous μCT study that observed reduced Tb.N., Tb.Th., Conn.D, and BV/TV, and increased Tb.Sp. in 3 months old SP deficient mice, compared to age matched wildtype controls [25]. A crucial difference between this study and the current one is that the SP deficient mice used in the previous study had undergone femur fractures 3 weeks prior to μCT analysis of the intact proximal femur contralateral to

the fracture side, and those data were compared to nonfracture wildtype control values. Femur fracture in WT mice induces systemic bone loss within 2 weeks of fracture, resulting in a 10% reduction in lumbar vertebrae BV/TV and a whole body reduction in bone mass density, and similar systemic bone loss changes also appear in fracture patients[26-28]. Furthermore, we previously observed that unilateral closed tibia fracture and casting for 4 weeks in 10-month-old skeletally mature rats reduced BV/TV in the contralateral distal femur [29-32], Collectively these data suggest that the skeletal architectural changes observed in the study using SP deficient fracture mice may be at least partially attributable to effects of post fracture systemic bone loss rather than SP deficiency.

By 5 months the SP deficient mice exhibited a decline in the proximal tibia cancellous bone volume fraction that was not observed in the wildtype mice (Fig. 3A). The loss of cancellous BV/TV was associated with a decrease in trabecular number and thickness in the SP deficient mice, in contrast to wildtype mice where aging was accompanied by a decrease in trabecular number and an increase in trabecular thickness (Fig.3B, C), in agreement with a prior study in wildtype mice [23].

Trabecular space increased with aging in both strains of mice, but to a greater extent in mice lacking SP (Fig. 3D). Trabecular connectivity decreased with aging in both SP deficient and wildtype mice (Fig. 3E), but there were no changes in cortical thickness in either mouse strain (Fig. 3F, Table 2). Interestingly, there was no loss of diaphyseal bone in the SP deficient mice, which may be attributable to the minimal peptidnergic innervation of cortical bone [18, 22, 33-35]. Continued periosteal expansion with aging in the mid-diaphyseal region is hypothesized to help to maintain whole bone bending strength in the face of endocortical resorption and deteriorating bone properties with age [24, 36]. Both strains of mice exhibited a significant decline in cortical bone area fraction and a significant increase in bone marrow cavity and cortical bone perimeter with aging, consistent with the previous reports in wildtype mice (Table 2)[24, 36]. Collectively, these findings of reduced trabecular bone volume and trabecular thickness, and increased trabecular space in 5 months old SP deficient mice, relative to age matched controls, support the hypothesis that SP signaling in cancellous bone inhibits the adverse effects of aging on bone mass, structure, and strength[5].

Consistent with the μCT data demonstrating no skeletal differences between SP deficient and wildtype mice at 2 months of age (Fig. 3, Table 2), no differences were observed in bone formation rates or osteoclast numbers per bone surface between SP deficient and wildtype mice at 2 months of age (Fig. 4). These results concur with those of a prior study showing no differences between wildtype and SP deficient mice regarding the numbers of runt-related transcription factor 2 (RUNX2) and TRAP labeled osteoblasts and osteoclasts in the proximal femoral metaphysis of 2 months old mice [21]. Furthermore, there were no differences in bone length or body weight between SP deficient and wildtype mice at 2 months of age (Fig. 1). Collectively, these results indicate that SP signaling does not contribute to developmental bone modeling.

The μCT findings of reduced trabecular bone volume and trabecular thickness, and increased trabecular space in the 5 months old SP deficient mice (*vs* wildtype mice, Fig. 3, Table 2)

concur with the histomorphometric data demonstrating a significant reduction in trabecular bone formation rates and increased osteoclast numbers per bone surface in 5 months old SP deficient mice, when compared age matched controls (Fig.4). In addition, the SP deficient mice had elevated urinary DPD levels, relative to wildtype controls, at both 2 and 5 months of age (Fig. 4E). These findings of reduced trabecular bone volume and thickness, increased trabecular space, decreased bone formation rates, increased osteoclast surface numbers, and accelerated bone resorption in aging SP deficient mice support the hypothesis that SP signaling stimulates cancellous bone formation and inhibits osteoclastogenesis and bone resorption in aging mice.

In agreement with the *in vivo* results demonstrating reduced trabecular bone volume and bone formation rates in aging SP deficient mice, previous *in vitro* studies have demonstrated that SP treatment increased the number and size of bone colonies, stimulated bone marrow stromal cell osteogenesis and osteoblastic cell differentiation [8, 17, 37]. Contrariwise to the *in vivo* results of the current study demonstrating increased osteoclastogenesis and bone resorption activity in aging SP deficient mice, previous *in vitro* studies had suggested that SP signaling stimulated osteoclastogenesis and bone resorption [8, 38, 39]. The reason for the divergent *in vivo* and *in vitro* effects of SP signaling on osteoclastogenesis and bone resorption are unknown, but similarly, CGRP deficient aging mice also exhibit divergent *in vitro* and *in vivo* osteoclast responses to neuropeptide signaling. The *in vitro* literature has consistently observed CGRP inhibition of osteoclastogenesis and bone resorption [7, 40-45], but aging CGRP deficient mice have no changes in osteoclast number per surface, osteoclast surface per bone surface, or urinary DPD levels [9].

Our previous study demonstrated that capsaicin sensitive unmyelinated sensory neurons contributed to skeletal homeostasis and that lesioning these neurons in aging rats reduced SP and CGRP levels in trabecular bone with subsequent loss of trabecular connectivity and thickness, reduced bone volume, and increased osteoclast number and surface [5]. Based on the results of the current study demonstrating increased osteoclastogenesis and bone resorption in aging SP deficient mice, and the normal osteoclastogenesis and bone resorption findings reported in aging CGRP deficient mice [9], we postulate that the increased osteoclastogenesis and loss of trabecular bone observed after lesioning sensory peptidenergic neurons is attributable to the loss of SP signaling in trabecular bone.

In the present study SP deficient mice were utilized to determine whether substance P signaling contributes to osteogenic bone reparation. Bone fracture healing is a regenerative process that restores bone structure and function through a process reflecting skeletal development and bone growth. The SP sensory neurons densely innervate the periosteum and bone marrow compartments [22] that are the main sources of osteogenitor cells. In this study, we observed that SP deficiency delayed cortical bone reparation by delaying bone callus formation during the earlier phase and delaying cortical bone remodeling process during the later phase of bone healing (Fig. 5). These results confirm and extend prior studies demonstrating; 1) a dramatic increase in SP innervation in fracture callus, peaking at 21 days post injury [46], 2) increased bone fragility after healing in fracture mice treated with capsaicin or with daily injections of an NK1 receptor antagonist [47, 48], and 3) a

decrease in bone callus osteoclast numbers and inferior mechanical properties after healing in SP deficient fracture mice [25].

In conclusion, the loss of SP signaling in aging mice caused a reduction in bone formation and increased resorption, with subsequent loss of metaphyseal bone. Reduced neuropeptide signaling is observed in a variety of conditions, including glucocorticoid use,[49, 50] aging [51-53], familial dysautonomia,[4], and nerve injuries [54, 55], and these heterogeneous conditions are associated osteopenia and increased fracture risk. We postulate that peptidnergic signaling is a crucial contributor to skeletal health and would be a novel therapeutic target for the treatment of osteoporosis in these conditions.

Acknowledgments

Funding sources: National Institutes of Health R01 (DK067197) and Veterans Affairs Merit (A4265R).

Abbreviations:

SP	substance P
DPD	deoxypyridinoline cross-links
CGRP	calcitonin gene-related peptide
BMD	bone mineral density
NK1	neurokinin 1 receptor
CRLR	calcitonin receptor-like receptor
RAMP1	receptor activity modifying protein 1
BMSCs	bone marrow stromal cells
BMMs	bone marrow macrophages
RANKL	nuclear factor-κB ligand
BV/TV%	bone volume fraction
Tb.N	trabecular number
Tb.Th	trabecular thickness
Tb.Sp	trabecular separation
ConnD	connectivity density
Tt.A	total cross-sectional area
B.Ar	cortical bone area
Ct.Th	cortical thickness
Me.Ar	medullary area

B.P	bone perimeter
B.Ar/T.Ar	relative cortical bone area
N.Oc/BS	number of osteoclasts per bone surface
BFR/BS	surface-based bone formation rate
Me. BV/TV	bone volume within the bone marrow cavity calculated as a percentage of the area of within the medullary cavity directly below the defect
Ct. BV/TV	bone volume within the cortical defect calculated as a percentage of the area of the cortical defect

References

1. Bjurholm A, et al., Substance P- and CGRP-immunoreactive nerves in bone. Peptides, 1988 9(1): p. 165–71. [PubMed: 2452430]
2. Maayan C, et al., Calcitonin gene related peptide in familial dysautonomia. Neuropeptides, 2001 35(3-4): p. 189–95. [PubMed: 11884210]
3. Pearson J, et al., The sural nerve in familial dysautonomia. J Neuropathol Exp Neurol, 1975 34(5): p. 413–24. [PubMed: 1176995]
4. Maayan C, et al., Bone mineral density and metabolism in familial dysautonomia. Osteoporos Int, 2002 13(5):p. 429–33. [PubMed: 12086355]
5. Offley SC, et al., Capsaicin-sensitive sensory neurons contribute to the maintenance of trabecular bone integrity. J Bone Miner Res, 2005 20(2):p. 257–67. [PubMed: 15647820]
6. Kingery WS, Davies MF, and Clark JD, A substance P receptor (NK1) antagonist can reverse vascular and nociceptive abnormalities in a rat model of complex regional pain syndrome type II. Pain, 2003 104(1-2): p. 75–84. [PubMed: 12855316]
7. Wang L, et al., Calcitonin-gene-related peptide stimulates stromal cell osteogenic differentiation and inhibits RANKL induced NF-kappaB activation, osteoclastogenesis and bone resorption. Bone, 2010 46(5): p. 1369–79. [PubMed: 19962460]
8. Wang L, et al., Substance P stimulates bone marrow stromal cell osteogenic activity, osteoclast differentiation, and resorption activity in vitro. Bone, 2009 45(2): p. 309–20. [PubMed: 19379851]
9. Schinke T, et al., Decreased bone formation and osteopenia in mice lacking alphacalcitonin gene-related peptide. J Bone Miner Res, 2004 19(12): p. 2049–56. [PubMed: 15537449]
10. Cao YQ, et al., Primary afferent tachykinins are required to experience moderate to intense pain. Nature, 1998 392(6674): p. 390–4. [PubMed: 9537322]
11. Huhtakangas JA, et al., The vitamin D receptor is present in caveolae-enriched plasma membranes and binds 1 alpha,25(OH)2-vitamin D3 in vivo and in vitro. Mol Endocrinol, 2004 18(11): p. 2660–71. [PubMed: 15272054]
12. Hildebrand T and Ruegsegger P, Quantification of Bone Microarchitecture with the Structure Model Index. Comput Methods Biomech Biomed Engin, 1997 1(1): p. 15–23. [PubMed: 11264794]
13. Hildebrand T, et al., Direct three-dimensional morphometric analysis of human cancellous bone: microstructural data from spine, femur, iliac crest, and calcaneus. J Bone Miner Res, 1999 14(7): p. 1167–74 [PubMed: 10404017]
14. Parfitt AM, et al., Bone histomorphometry: standardization of nomenclature, symbols, and units. Report of the ASBMR Histomorphometry Nomenclature Committee. J Bone Miner Res, 1987 2(6): p. 595–610. [PubMed: 3455637]
15. Behr B, et al., Fgf-9 is required for angiogenesis and osteogenesis in long bone repair. Proc Natl Acad Sci U S A, 2010 107(26): p. 11853–8. [PubMed: 20547837]

16. Togari A, et al., Expression of mRNAs for neuropeptide receptors and beta-adrenergic receptors in human osteoblasts and human osteogenic sarcoma cells. Neurosci Lett, 1997 233(2-3): p. 125–8. [PubMed: 9350848]
17. Goto T, et al., Substance P stimulates late-stage rat osteoblastic bone formation through neurokinin-1 receptors. Neuropeptides, 2007 41(1): p. 25–31. [PubMed: 17204323]
18. Goto T, et al., Light- and electron-microscopic study of the distribution of axons containing substance P and the localization of neurokinin-1 receptor in bone. Cell Tissue Res, 1998 293(1): p. 87–93. [PubMed: 9634600]
19. Liu HJ, et al., Substance P Promotes the Proliferation, but Inhibits Differentiation and Mineralization of Osteoblasts from Rats with Spinal Cord Injury via RANKL/OPG System. PLoS One, 2016 11(10): p. e0165063. [PubMed: 27764190]
20. Nagao S, et al., Expression of neuropeptide receptor mRNA during osteoblastic differentiation of mouse iPS cells. Neuropeptides, 2014 48(6): p. 399–406. [PubMed: 25464890]
21. Niedermair T, et al., Substance P modulates bone remodeling properties of murine osteoblasts and osteoclasts. Sci Rep, 2018 8(1): p. 9199. [PubMed: 29907830]
22. Mach DB, et al., Origins of skeletal pain: sensory and sympathetic innervation of the mouse femur. Neuroscience, 2002 113(1): p. 155–66. [PubMed: 12123694]
23. Halloran BP, et al., Changes in bone structure and mass with advancing age in the male C57BL/6J mouse. J Bone Miner Res, 2002 17(6): p. 1044–50. [PubMed: 12054159]
24. Glatt V, et al., Age-related changes in trabecular architecture differ in female and male C57BL/6J mice. J Bone Miner Res, 2007 22(8): p. 1197–207. [PubMed: 17488199]
25. Niedermair T, et al., Absence of substance P and the sympathetic nervous system impact on bone structure and chondrocyte differentiation in an adult model of endochondral ossification. Matrix Biol, 2014 38: p. 22–35. [PubMed: 25063231]
26. Ely EV, et al., Region-dependent bone loss in the lumbar spine following femoral fracture in mice. Bone, 2020 140: p. 115555. [PubMed: 32736144]
27. Emami AJ, et al., Age Dependence of Systemic Bone Loss and Recovery Following Femur Fracture in Mice. J Bone Miner Res, 2019 34(1): p. 157–170. [PubMed: 30189111]
28. Osipov B, Emami AJ, and Christiansen BA, Systemic Bone Loss After Fracture. Clin Rev Bone Miner Metab, 2018 16(4): p. 116–130. [PubMed: 31363348]
29. Wei T, et al., Pentoxifylline attenuates nociceptive sensitization and cytokine expression in a tibia fracture rat model of complex regional pain syndrome. Eur J Pain, 2009 13(3): p. 253–62. [PubMed: 18554967]
30. Li WW, et al., The role of enhanced cutaneous IL-1beta signaling in a rat tibia fracture model of complex regional pain syndrome. Pain, 2009 144(3): p. 303–13. [PubMed: 19473768]
31. Sabsovich I, et al., Effect of anti-NGF antibodies in a rat tibia fracture model of complex regional pain syndrome type I. Pain, 2008 138(1): p. 47–60. [PubMed: 18083307]
32. Wang L, et al., Bisphosphonates Inhibit Pain, Bone Loss, and Inflammation in a Rat Tibia Fracture Model of Complex Regional Pain Syndrome. Anesth Analg, 2016 123(4): p. 1033–45. [PubMed: 27636578]
33. Bjurholm A, Neuroendocrine peptides in bone. Int Orthop, 1991 15(4): p. 325–9. [PubMed: 1725676]
34. Hukkanen M, et al., Innervation of bone from healthy and arthritic rats by substance P and calcitonin gene related peptide containing sensory fibers. J Rheumatol, 1992 19(8): p. 1252–9. [PubMed: 1383542]
35. Irie K, et al., Calcitonin gene-related peptide (CGRP)-containing nerve fibers in bone tissue and their involvement in bone remodeling. Microsc Res Tech, 2002 58(2): p. 85–90. [PubMed: 12203707]
36. Seeman E, Periosteal bone formation--a neglected determinant of bone strength. N Engl J Med, 2003 349(4): p. 320–3. [PubMed: 12878736]
37. Shih C and Bernard GW, Neurogenic substance P stimulates osteogenesis in vitro. Peptides, 1997 18(2): p. 323–6. [PubMed: 9149307]

38. Mori T, et al., Substance P regulates the function of rabbit cultured osteoclast; increase of intracellular free calcium concentration and enhancement of bone resorption. Biochem Biophys Res Commun, 1999 262(2): p. 418–22. [PubMed: 10462490]
39. Sohn SJ, Substance P upregulates osteoclastogenesis by activating nuclear factor kappa B in osteoclast precursors. Acta Otolaryngol, 2005 125(2): p. 130–3. [PubMed: 15880941]
40. Akopian A, et al., Effects of CGRP on human osteoclast-like cell formation: a possible connection with the bone loss in neurological disorders? Peptides, 2000 21(4): p. 559–64. [PubMed: 10822112]
41. Cornish J, et al., Effects of calcitonin, amylin, and calcitonin gene-related peptide on osteoclast development. Bone, 2001 29(2): p. 162–8. [PubMed: 11502478]
42. Owan I and Ibaraki K, The role of calcitonin gene-related peptide (CGRP) in macrophages: the presence of functional receptors and effects on proliferation and differentiation into osteoclast-like cells. Bone Miner, 1994 24(2): p. 151–64. [PubMed: 8199534]
43. Ishizuka K, et al., Inhibitory effect of CGRP on osteoclast formation by mouse bone marrow cells treated with isoproterenol. Neurosci Lett, 2005 379(1): p. 47–51. [PubMed: 15814197]
44. Alam AS, et al., Amylin inhibits bone resorption by a direct effect on the motility of rat osteoclasts. Exp Physiol, 1993 78(2): p. 183–96. [PubMed: 8385961]
45. Zaidi M, et al., A direct action of human calcitonin gene-related peptide on isolated osteoclasts. J Endocrinol, 1987 115(3): p. 511–8. [PubMed: 3502132]
46. Li J, et al., Occurrence of substance P in bone repair under different load comparison of straight and angulated fracture in rat tibia. J Orthop Res, 2010 28(12): p. 1643–50. [PubMed: 20540103]
47. Apel PJ, et al., Effect of selective sensory denervation on fracture-healing: an experimental study of rats. J Bone Joint Surg Am, 2009 91(12): p. 2886–95. [PubMed: 19952252]
48. Hofman M, et al., Effect of neurokinin-1-receptor blockage on fracture healing in rats. Sci Rep, 2019 9(1): p. 9744. [PubMed: 31278316]
49. Kingery WS, et al., Glucocorticoid inhibition of neuropathic limb edema and cutaneous neurogenic extravasation. Brain Res, 2001 913(2): p. 140–8. [PubMed: 11549377]
50. Manolagas SC and Weinstein RS, New developments in the pathogenesis and treatment of steroid-induced osteoporosis. J Bone Miner Res, 1999 14(7): p. 1061–6. [PubMed: 10404005]
51. Kiebzak GM, et al., Bone status of senescent male rats: chemical, morphometric, and mechanical analysis. J Bone Miner Res, 1988 3(1): p. 37–45. [PubMed: 3264993]
52. Wang L, et al., Male rodent model of age-related bone loss in men. Bone, 2001 29(2): p. 141–8. [PubMed: 11502475]
53. Bergman E, et al., Neuropeptides and neurotrophin receptor mRNAs in primary sensory neurons of aged rats. J Comp Neurol, 1996 375(2): p. 303–19. [PubMed: 8915832]
54. Kingery WS, et al., A substance P receptor (NK1) antagonist enhances the widespread osteoporotic effects of sciatic nerve section. Bone, 2003 33(6): p. 927–36. [PubMed: 14678852]
55. Scott C, et al., Capsaicin-sensitive afferents are involved in signalling transneuronal effects between cutaneous sensory nerves. Neuroscience, 2000 95(2): p. 535–41. [PubMed: 10658634]

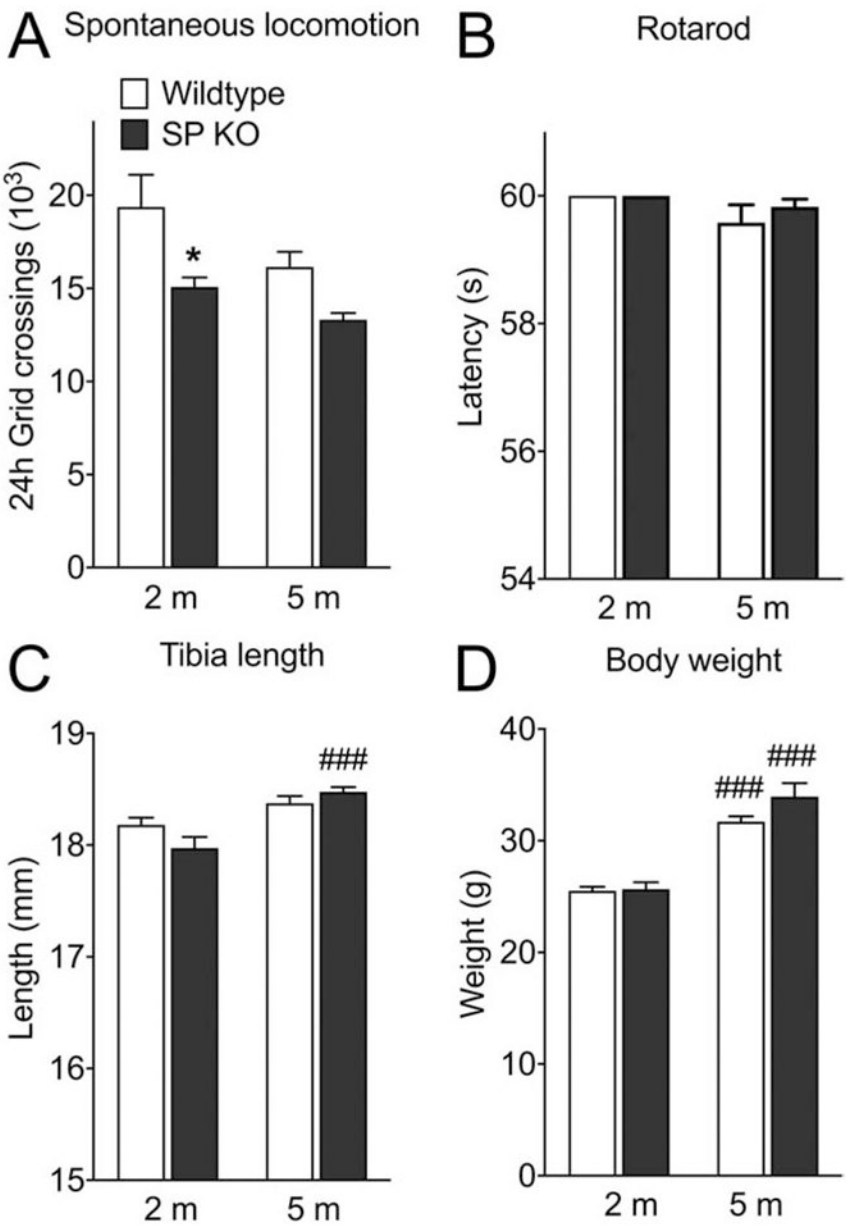

Figure 1.

There was no evidence of skeletal unloading in substance P (SP) deficient mice. Spontaneous 24-hour locomotor activity (A) was slightly reduced in 2 month-old SP deficient mice, compared to wildtype mice, but by 5 months of age there were no significant differences between groups. As measured by rotarod testing (B), there were no differences in motor strength and coordination between strains at 2 and 5 months of age. No significant differences in tibia length (C) or body weight (D) were observed between SP deficient and wildtype mice at 2 or 5 months of age, but tibia length and body weight did increase with aging. Data are expressed as mean values ± SEM., n = 13-15 per cohort. * $p<0.05$ *vs* age matched wildtype mice, ###$p<0.001$ *vs* 2 month old strain matched mice. 2m: 2 months old, 5m: 5 months old, SP KO: Substance P deficient mice, Wildtype: wildtype control mice

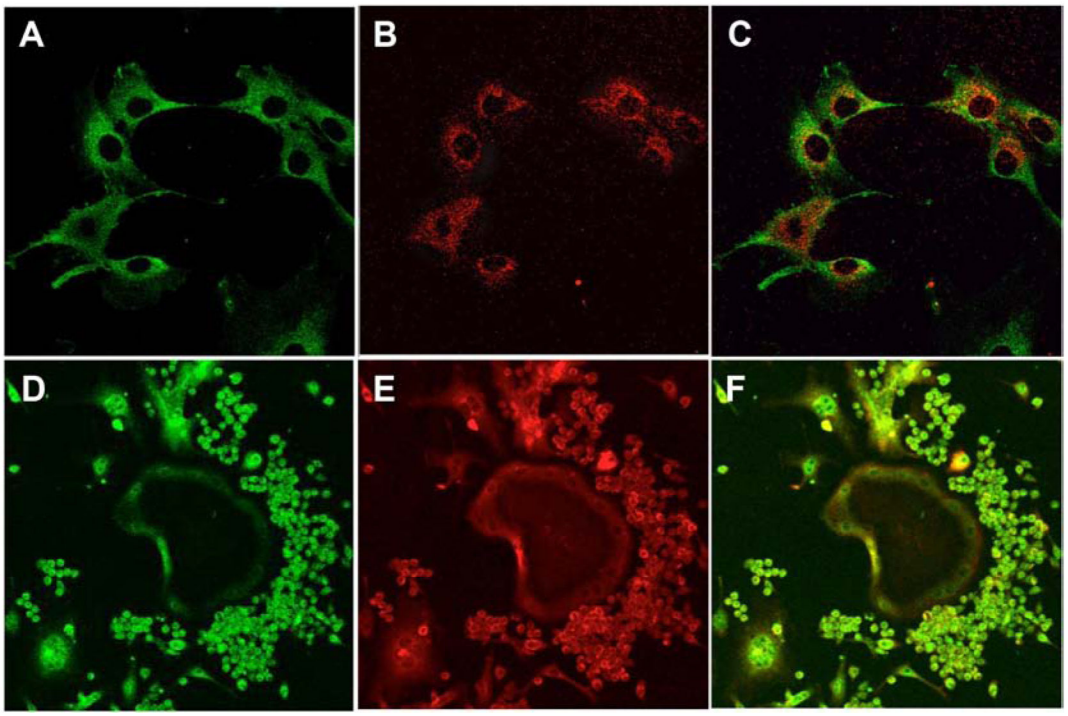

Figure 2.

Immunostaining confirms the presence of the SP neurokinin 1 receptor (NK1-R) in the MC3T3-E1 osteoblastic cell line (upper panel, x400) and in the RANKL stimulated Raw 264.7 osteoclastic cell line (lower panel, x20). Harvested MC3T3-E1 and RAW 264.7 cells were permeabilized and then co-stained for the presence of either alkaline phosphatase (green, A) and NK1-Rs (red, B), or tartrate-resistant acid phosphatase (TRAP, green, D) and NK1-Rs (red, E), respectively. Note that NK1-R labeling was observed in the cytoplasm and on the cell membrane of both types of bone cells. Images of C and F show the co-localization of NK-1Rs with alkaline phosphatase in osteoblasts (C) or with TRAP in osteoclasts and their progenitor cells (F)

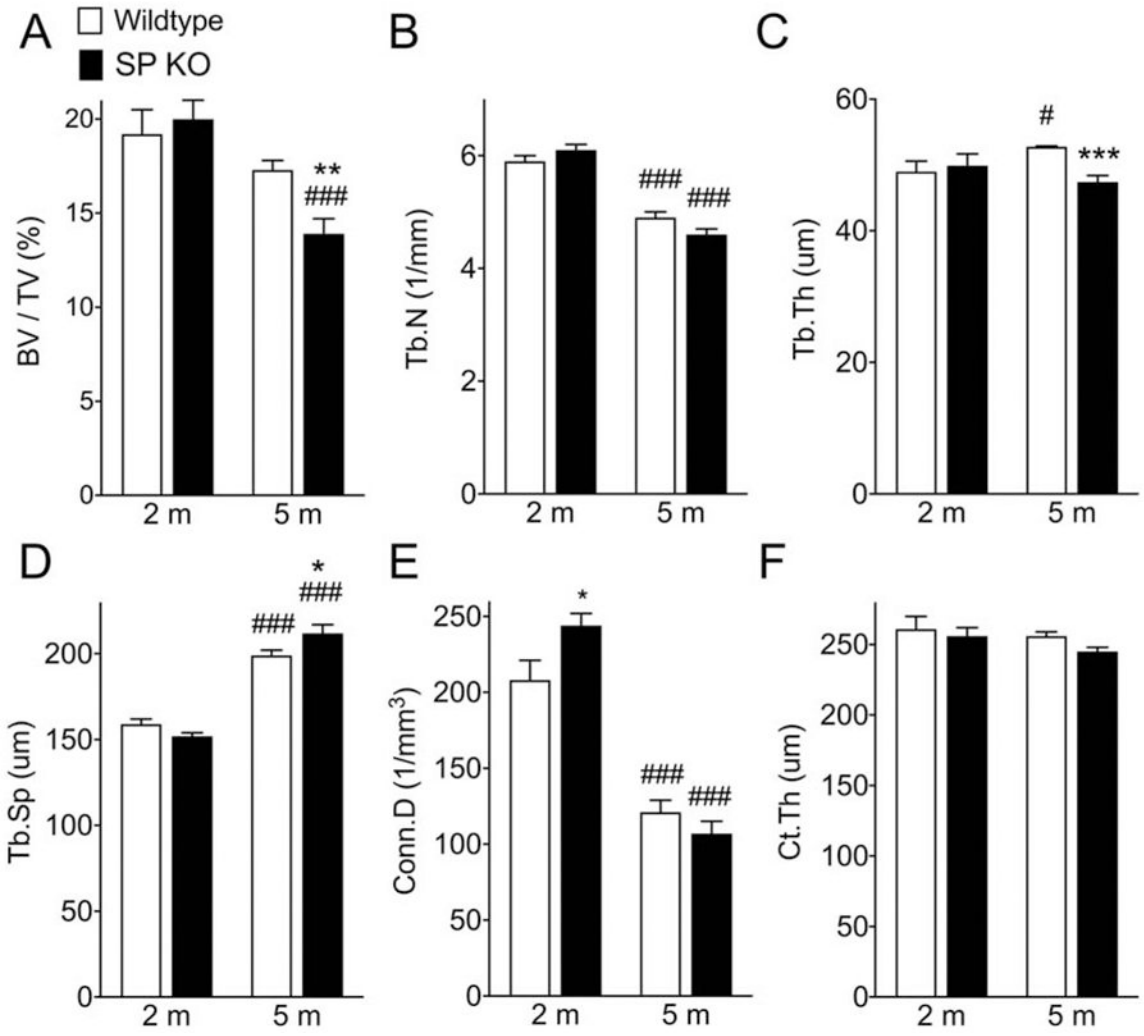

Figure 3.

SP deficient mice had accelerated cancellous bone loss with aging. MicroCT was used to evaluate cancellous bone architecture in the proximal tibia and cortical bone morphology at the tibia-fibular junction in SP deficient and wildtype control mice at both 2 and 5 months of age. No differences were observed in proximal tibia BV/TV (A), Tb.N (B), Tb.Th (C), Tb.Sp (D) and tibial-fibular junction Ct.Th (F) between 2 months old SP deficient mice and the age-matched controls. Aging wildtype mice had diminished Tb.N, and Conn.D (E) and increased TB.Sp, while aging SP deficient mice had reduced BV/TV, Tb.N, and Conn.D, and increased Tb.Sp. At 5 months of age the SP deficient mice, relative to age-matched wildtype mice, had decreased BV/TV and Tb.Th, with increased Tb.Sp. Data are expressed as mean values ± SEM., n = 10-12 per cohort. * $p<0.05$, ** $p<0.01$, *** $p<0.001$ *vs* age matched wildtype mice, ## $p<0.1$, ### $p<0.001$ *vs* 2 month old strain matched mice. 2m: 2 months old, 5m: 5 months old, SP KO: Substance P deficient mice, Wildtype: wildtype control mice

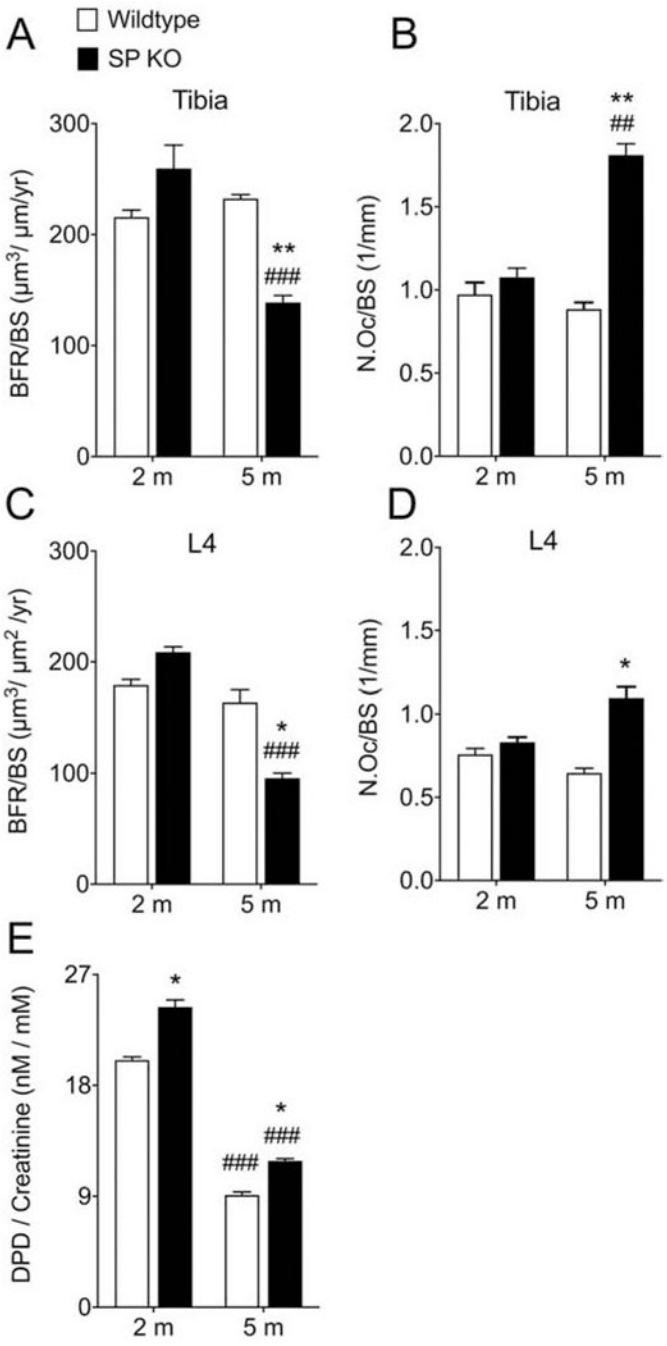

Figure 4.

SP deficient mice exhibit diminished trabecular bone formation, increased osteoclast numbers, and increased bone resorption with aging. To characterize the effects of aging on bone remodeling activity in SP-deficient mice, we assessed changes in bone formation rateand osteoclast numbers at the trabecular bone surfaces in the proximal tibia (A,B) and L4 vertebral body (C,D) between the ages of 2 and 5 months. An age-related decrease in cancellous bone formation rate (BFR/BS) and an age-related increase in osteoclastogenesis, as indicated by osteoclast surface numbers (N.Oc/BS), were observed in SP deficient mice,

but not in wildtype controls. At the age of 5 months, cancellous bone formation rate was significantly lower whereas osteoclast number was significantly higher in the SP deficient mice than in the age-matched wildtype controls. Bone resorption was also studied by measuring the total urinary DPD levels. Urinary DPD levels were reduced in both strains from 2 to 5 months of age (E). However, at both 2 and 5 months of age the DPD levels in SP deficient mice were significantly higher than in the age-matched wildtype controls. Data are expressed as mean values ± SEM., n = 10-12 per cohort. * $p<0.05$, ** $p<0.01$, *** $p<0.001$ *vs* age matched wildtype mice, ## $p<0.1$, ### $p<0.001$ *vs* 2 month old strain matched mice. 2m: 2 months old, 5m: 5 months old, SP KO: Substance P deficient mice, Wildtype: wildtype control mice

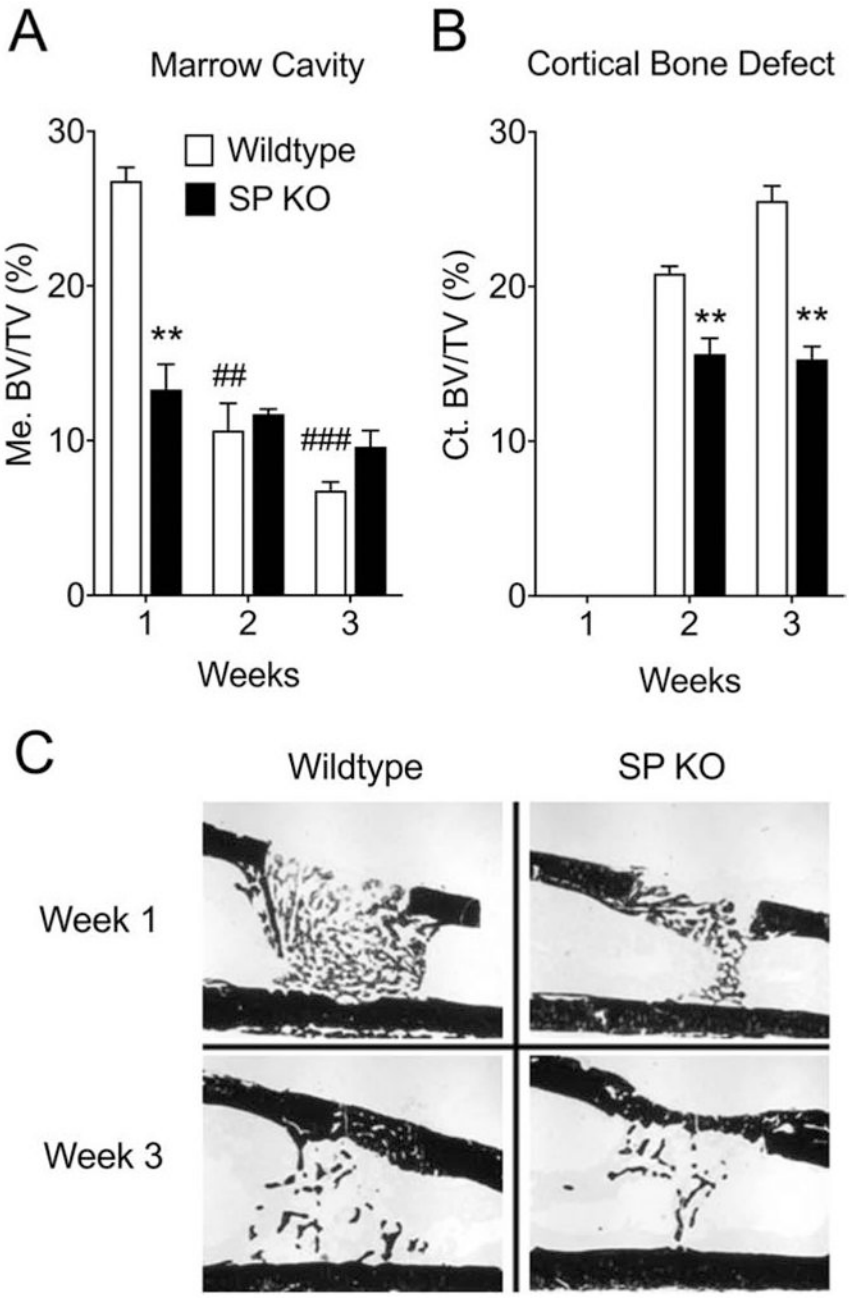

Figure 5.

SP deficient mice had delayed cortical bone reparation. A 1mm hole was drilled through cortical bone and bone marrow, leaving the opposite cortex intact, thus generating a model of stabilized fracture healing. Histomorphometry was used to evaluate bone regeneration in the marrow cavity and cortex of SP deficient and wildtype control mice at 1, 2, and 3 weeks post surgery. Regenerating woven bone appeared in the marrow area within 1 week after cortical defect surgery in both strains of mice and persisted for at least 3 weeks post surgery (A,C). The bony callous volume within bone marrow cavity zone (Me. BV/TV) at 1-week post surgery was significantly less in the SP deficient *vs* wildtype mice. Lamellar bone and periosteal fibrous tissue appeared at the cortical bone defect region at 2 and 3 weeks post

surgery (B,C). The bone callous volume within cortical defect zone (Ct. BV/TV) was reduced in the SP deficient mice *vs* wildtype controls at both 2 and 3 weeks post surgery. Data are expressed as mean values ± SEM., n = 6-8 per cohort. **p<0.01 *vs* age matched wildtype mice, ##p<0.1, ###p<0.001 *vs* 1 week post surgery strain matched mice, SP KO: Substance P deficient mice, Wildtype: wildtype control mice

Table 1.

Serum chemistry in 2 and 5 months-old wildtype and substance P deficient (SP KO) mice.

	2 months		5 months	
	Wildlype	**SP KO**	**Wildtype**	**SP KO**
calcium (mg/dL)	8.86 ±0.08	8.89 ±0.05	8.86 ±0.06	8.79 ±0.07
phosphorus (mg/dL)	8.47 ±0.23	7.84 ±0.28	6.96 ±0.25	6.32 ±0.26
sodium (mmol/L)	145.9 ±0.9	147.3 ±0.5	147.7 ±0.6	149.4 ±0.47
potassium (mmol/L)	5.56 ±0.12	5.19 ± 0.11	5.34 ±0.14	5.08 ±0.15
chloride (mmol/L)	111.6 ± 1.2	113.3 ± 1.1	110.9 ±0.6	113.6 ±0.71
glucose (mg/dL)	251.4 ± 18.8	275.7 ± 17.6	240.6 ±5.9	256.0 ±8.52
blood urea nitrogen (mg/dL)	22.6 ± 1.3	19.5 ± 1.8	18.9 ±0.7	17.4 ±1.18
creatinine (mg/dL)	0.19 ±0.01	0.15 ±0.01	0.14 ±0.01	0.12 ±0.01
albumin (g/dL)	1.39 ±0.04	1.46 ±0.03	1.29 ±0.02	1.24 ±0.03
total protein (g/dL)	4.12 ±0.08	4.24 ±0.06	3.99 ±0.06	3.89 ±0.06
cholesterol (mg/dL)	88.9 ±6.4	100.3 ±3.5	110.5 ±2.2	**92.7 ± 2.76*****
alkaline phosphatase (IU/L)	50.4 ± 1.6	56.1 ± 4.9	50.4 ± 1.6	56.1 ± 4.92
alanine transaminase (IU/L)	26.6 ± 2.3	47.3 ± 14.6	26.5 ± 2.0	35.4 ± 5.08
aspartate transaminase (IU/L)	179.1 ± 22.0	142.9 ± 23.2	171.4 ± 21.8	171.0 ± 21.0
γ-glutamyl transpeptidase (IU/L)	5.33 ± 0.59	6.29 ± 0.81	6.60 ± 0.66	7.62 ± 0.50
total bilirubin (mg/dL)	0.49 ± 0.05	0.51 ± 0.04	0.44 ± 0.03	0.41 ± 0.04
creatinine phosphokinase (IU/L)	601.2 ± 72.7	540.7 ± 45.1	646.7 ± 84.0	562.5 ± 61.3

Bold font indicates significant value differences between wildtype and substance P deficient (SP KO) mice of the same age (mean ± SE, n = 14-15 per cohort).

*** $p < 0.001$

Table 2.

MicroCT skeletal morphology in 2 and 5 months-old wild type and SP deficient (SP KO) mice.

	Wildtype			SPKO		
	2 months	**5 months**	**MPD**	**2 months**	**5 months**	**MPD**
Proximal tibia						
BV/TV (%)	19.2 ± 1.3	17.3 ± 0.5	−9.4%	20 ± 1	13.9 ± 0.8	**−30.7%** *
Tb.N (mm^{-1})	5.9 ± 0.1	4.9 ± 0.1	−18.4%	6.1 ± 0.1	4.6 ± 0.1	**−24.7%** *
Tb.Th (μm)	49 ± 1.6	52.8 ± 0.9	7.7%	49.9 ± 1.8	47.4 ± 1	**−5%** *
Tb.Sp (μm)	159 ±3	199 ±3	25%	152 ±2	212 ±5	**38.8%** *
Conn.D ($1/mm^3$)	208 ± 13	121 ± 8	−41.9%	244 ± 8	107 ± 8	**−56.2%** **
Tibial-fibular junction						
B.Ar (mm^2)	0.69 ± 0.03	0.72 ± 0.01	4.2%	0.65 ± 0.02	0.70 ± 0.02	7.6%
Tt.Ar (mm^2)	0.98 ± 0.03	1.07 ± 0.02	9.7%	0.92 ± 0.02	1.09 ± 0.03	18.7%
Me.Ar (mm^2)	0.28 ± 0.01	0.36 ± 0.02	26%	0.27 ± 0.01	0.39 ± 0.01	45.8%
Ct.Th (μm)	261 ± 9	256 ± 3	−1.8%	256 ± 6	245 ± 3	−4.3%
B.Pm (mn)	5.7 ± 0.1	6.0 ± 0.1	6.6%	5.5 ± 0.1	6.2 ± 0.1	**13%** *
B.Ar/Tt.Ar (%)	70.7 ± 1	67.4 ± 0.8	−4.6%	71 ± 0.9	64.5 ± 0.7	−9.1%

The effects of aging on trabecular and cortical bone parameters in wildtype and substance P deficient (SP KO) mice are expressed as the Mean Percent Difference (MPD). MPD = ((5 months - 2 months) / 2 months) x 100. Bold font indicates significant differences in MPD between SP KO and wildtype mice (n=14-15 per cohort).

* $p < 0.05$,

** $p < 0.01$